



## Seismic Safety Evaluation Based on Muon Monitoring of Prambanan World Heritage Temple Damaged by 2006 Central Java Earthquake, Indonesia

T. Hanazato<sup>(1)</sup>, H. Tanaka<sup>(2)</sup>, T. Kusagaya<sup>(3)</sup>, Y. Okamoto<sup>(4)</sup>, Y. Uekita<sup>(5)</sup> and Y. Subroto<sup>(6)</sup>

<sup>(1)</sup> Professor, Division of Architecture, Graduate School of Engineering, Mie University, hanazato@arch.mie-u.ac.jp

<sup>(2)</sup> Professor, Earthquake Research Institute, University of Tokyo, ht@eri.u-tokyo.ac.jp

<sup>(3)</sup> Ph.D. Student, Earthquake Research Institute, University of Tokyo, kusagaya@eri.u-tokyo.ac.jp

<sup>(4)</sup> Espace Architectural Design Office, Graduated Student from Mie University, okamoto@espace-ao.com

<sup>(5)</sup> Professor, World Heritage Studies Program, Faculty of Art and Design, Tsukuba University, uekita@heritage.tsukuba.ac.jp

<sup>(6)</sup> Professor, Faculty of Engineering Office, Gadjah Mada University, yoyok\_subroto@yahoo.com

### Abstract

Muon cosmic-ray that can penetrate rocks and soils gives us projection of the path' density, therefore, muography technology has been successfully developed in the geological field for disaster prevention of volcano explosion. Furthermore, it was utilized to survey the inner condition of a blast furnace in a steel mill during its operation time. On the other hand, non-destructive tests are required, in general, to conduct structural survey of heritage structures with cultural and historical values. In particular, when World Heritage Monuments are surveyed, we have to follow this principle strictly. There are a number of World Cultural Heritages of masonry in seismic regions in the World. When their seismic safety is assessed, seismic structural survey must be conducted by employing non-destructive tests. Considering that muography technology can be useful for structural survey of massive masonry structures as a non-destructive test, we installed the muon detecting equipment at the Prambanan Temples, World Cultural Heritage of stone masonry in Indonesia. The muon cosmic-ray was monitored for 5 months.

The Prambanan Temples of stone masonry structures were severely damaged by Central Java Earthquake of 2006. We had been successfully involved in architectural and structural survey project conducted by an international and interdisciplinary team. The damaged masonry monuments have been restored after the earthquake, however, restoration work of Candi Siva, the oldest and highest monument of the Prambanan Temples, had been delayed in starting, as the information of its inner structural condition was insufficient for proposing restoration plan. From an earthquake engineering point of view, 3-D finite element model was available for seismic structural diagnosis of such massive masonry structures. The scope of the present paper is to describe this challengeable non-destructive test utilizing muography technology for the Prambanan restoration project, as well as, to demonstrate applicability of this advanced technology to structural survey of World Cultural Heritages of masonry. Furthermore, the present paper demonstrates that this advanced technology will be useful for seismic safety evaluation. The muon data obtained at the site indicated that the monument must have inner chambers that had been unknown. The recorded data also indicated their sizes and locations. On the basis of this muography, the 3-D finite element model was revised to evaluate seismic safety of the monument. In the present study, not only the structure but also the soils were modeled to take into account the soli-structure interaction. It should be recognized that the Prambanan Temples were reconstructed by introducing RCC structure in by Dutch engineers in 1950's and Indonesian experts in 1990's. The analysis indicated that the inner structure of both masonry and RCC would not severely damaged, as the induced stress was less than the allowable stress. The present study demonstrates the muography will be useful for structural survey for seismic evaluation of heritage structures of masonry.

*Keywords: Muon, Non-destructive Test, Masonry, Heritage Structure, Seismic Safety Evaluation*

## 1. Introduction

The Prambanan Temples, the World Cultural Heritage of stone masonry structures were originally built in the 9th century in the suburbs at the historic city, Yogyakarta, in Java, Indonesia. Today, they are composed of existing 8 monuments, shown in Photo.1. Candi Siva, the object of the present research, is the largest structure in the site. Although they had ruined during their long histories, their structures were reconstructed in 20th century. Candi Siva was reconstructed first by Dutch engineers by introducing reinforced concrete structure in the middle of 20th century; the other buildings were reconstructed by Indonesian engineers during the end of 1980s and beginning of 1990s by employing the reinforced concrete technology introduced by Dutch engineers. In 1993, just after completion of reconstruction, those heritages were inscribed in World Cultural Heritage List. As mentioned above, the stone monuments were rebuilt by introducing inner concrete structures composed of reinforced concrete frames and infill rubble materials. The reinforced concrete frame was employed to confine infill rubble material structure for ensuring structural stability [1][2][3].

The Central Java Earthquake occurred on May 27, 2006. This devastating earthquake of magnitude (Mw) 6.4 affected various structural types of architectural heritages in and around the historic city of Yogyakarta which locates 25km from the epicenter. The Prambanan Temples were severely damaged by the ground motions generated by this near-field earthquake. In response to the emergency request by the Indonesian Government, Japanese Government dispatched an interdisciplinary expert team just after the earthquake in order to assess the earthquake damage to the Prambanan Temple for starting the restoration project. Following the cooperation program by Japanese Government for two years, the Japan- Indonesia international collaborative study on the seismic safety and structural stability of this damaged World Heritage structure started, which had been performed for about 4 years. During this scientific research program, the monitoring of earthquake and crack displacement had been carried out to verify the present structural stability. In addition, seismic response analyses were successfully performed by using both the simplified lumped masses and the 3-dimensional finite element models[4]. In those analytical studies, soil-structure interaction effect was taken into account, as dynamic behaviors of such massive rigid structure are significantly affected by soil-structure interaction. However, the inner structural condition of Candi Siva had been actually unknown, because of lack of the detailed drawings and of insufficient documents describing its internal structure for its reconstruction in 1950's. The finite element model in the initial study was made from the analysis model of Candi Hangsa/Garuda of which drawings were found on the assumption that the inner structure of Candi Siva was similar to that of Candi Hangsa/Garuda. Therefore, the analysis model of Candi Siva in the past studies was not based on the accurate information of the inner structure. In particular, the size of the inner hidden room in the roof of Candi Siva should be needed to be clarified for seismic diagnosis of the structure. This aspect implied necessity for the accurate internal structural condition of Candi Siva in order to provide more appropriate analysis model.



Photo. 1 - Prambanan Temple

As World Heritage monuments must require non-destructive tests employed for their structural survey, we introduced muon radiography technology that has been successfully developed to survey cross sections of volcanos and hidden active faults for disaster prevention [4]. This advanced technology was recently applied to survey the inner condition of a blast furnace in a steel mill during its operation time. Furthermore, it was reported that this technology was introduced to survey the nuclear reactor core meltdown at Fukushima Daiichi Plant damaged by 2011 East Japan Great Earthquake. Muon cosmic-ray can penetrate rocks and soils with thickness of km, which gives us projection of the path's density. For survey of inner structural condition of massive masonry monuments such as Prambanan Temple, muon radiography technology might be useful. In the present study, we employed this technology to measure the size of the hidden room of the upper part of Candi Siva. After identification of the size of the hidden room by the muography, the analysis model utilizing 3-D finite elements employed in our past study was revised. By using the revised analysis model that was more

reliable and accurate one than the past model, seismic response analysis was performed to assess seismic safety of Candi Siva.

## 2. Muography

### 2.1 Muon Monitoring Method

Figs. 1 and 2 show the muon-detecting system utilized in the present study and how to detect the muon by scintillators, respectively. The muon-detecting equipment was installed at the NW corner of the central room on the base floor where the statue of Siva was enshrined, shown in Figs.2 and 3. Candi Siva was imaged muographically by utilizing a detector with an active area of 1764cm<sup>2</sup> and with an angular interval of 70mrad. Fig.4 describes the cross-sectional view of the structure and radiant angle from the equipment.

In order to correct the detector characteristics, we considered the ratio of the data before a rotation to those after 180 degrees rotation. The monitoring period was between Oct. 18, 2013 and Feb. 13, 2014. In this period, the detector was rotated at 180 degrees around the vertical axis.

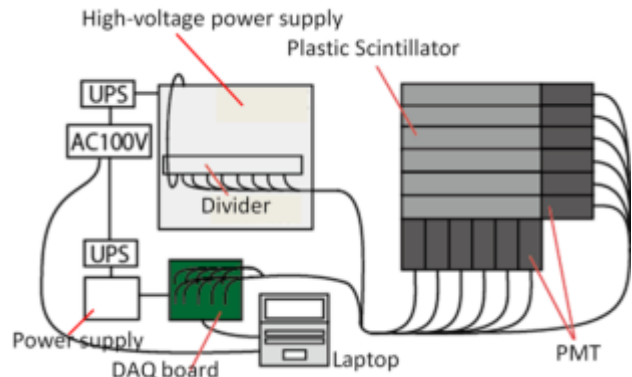


Fig.1 - Muon detecting system

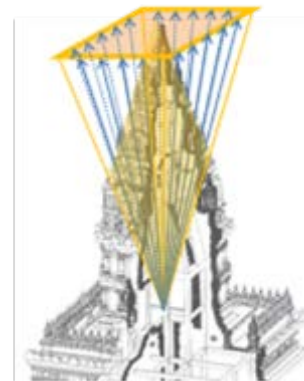
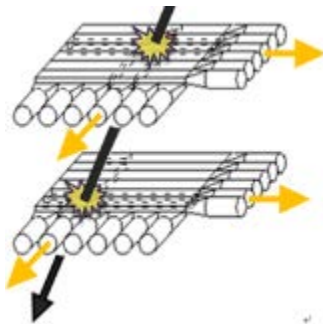


Fig.2 - Muon detection by scintillator and system installed

Fig.3 - Direction of muon detection

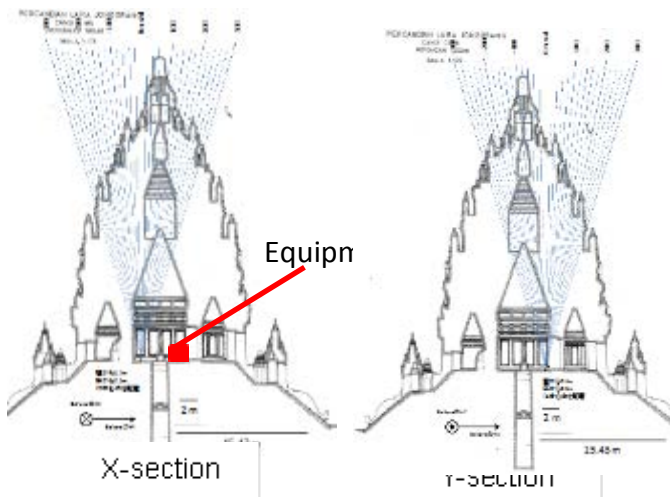
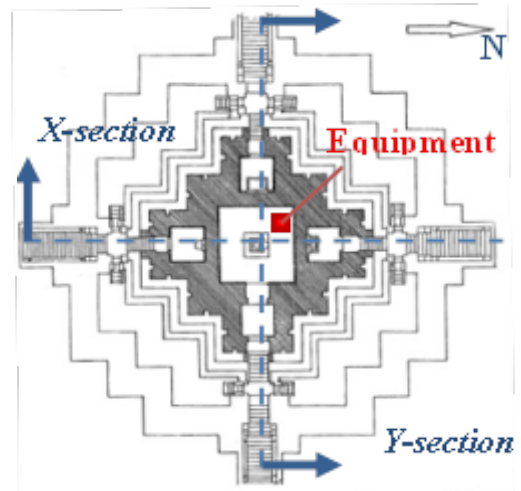


Fig.4 - Location of equipment and radiant angle for measurement



## 2.2 Simulation models

In the muography technology, comparison of the theoretical simulation and the monitored data can give the most reliable model of the structure. Therefore, simulation utilizing the assumed models was performed. In our simulation, a total of 6 models were assumed as followings on the basis of the roughly drawn old sketch that was kept at the restoration office ;

- 1) There was no hidden room in the upper part of the structure (we called 0-volume model)
- 2) There was a hidden room with a half volume shown in the drawing of the section (we called 0.5-volume model)
- 3) There was a hidden room with the same volume shown in the drawing of the section (we called 1-volume model)
- 4) There was a hidden room with double volume shown in the drawing of the section (we called 2-volume model)
- 5) There was a hidden room with triple volume shown in the drawing of the section (we called 3-volume model)
- 6) There was a hidden room with 4 times volume shown in the drawing of the section (we called 4-volume model)

In the present models, the basic 1-volume model was assumed as 5m cube with volume of 113m<sup>3</sup>, which was shown in the section roughly drawn when Candi Siva was reconstructed in the beginning of 1950's, shown in Fig.5. For examples, 0.5-Volume, 1-volume and 2 volume models are described in Fig. 7. In each model, path length (length of penetration of muon in structural material) should be evaluated, shown in Fig.6. For simulation, a grid of 0.5m cube was utilized to calculate the path length. Also, the bulk density of the structural materials was estimated by the following equation;

$$\rho = \frac{\rho_1 V_1 + \rho_2 V_2}{V_1 + V_2} \quad (1)$$

Hence,  $\rho$  : bulk density

$\rho_1$  : Density of structural materials  
( stone and concrete materials 2000kg/m<sup>3</sup>)

$\rho_2$  : Density of air in the room  
(1.18kg/m<sup>3</sup> at temperature of 25 °C)

$V_1$  : Bulk volume of materials in one angular segment

$V_2$  : Bulk volume of air in the room in one angular segment

Theoretical simulation was performed by using the above models. It is well known, the muon is actually flied from space randomly in any direction. In the present study, probabilistic approach was applied.

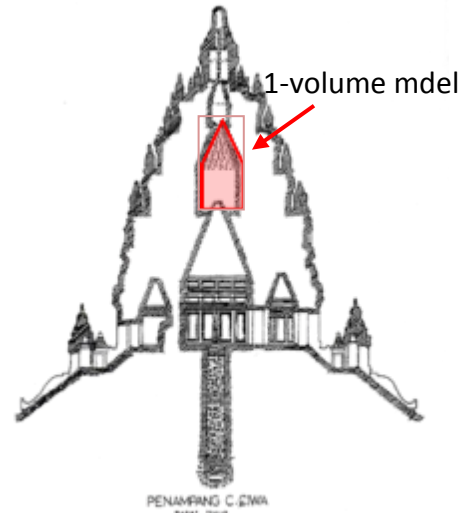


Fig.5 - 1-Volume model for simulation

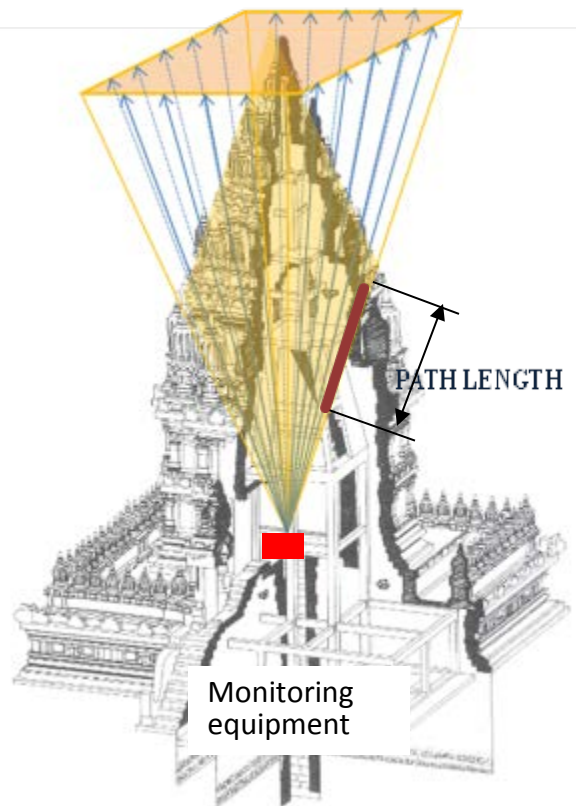


Fig.6 - Calculation of path length

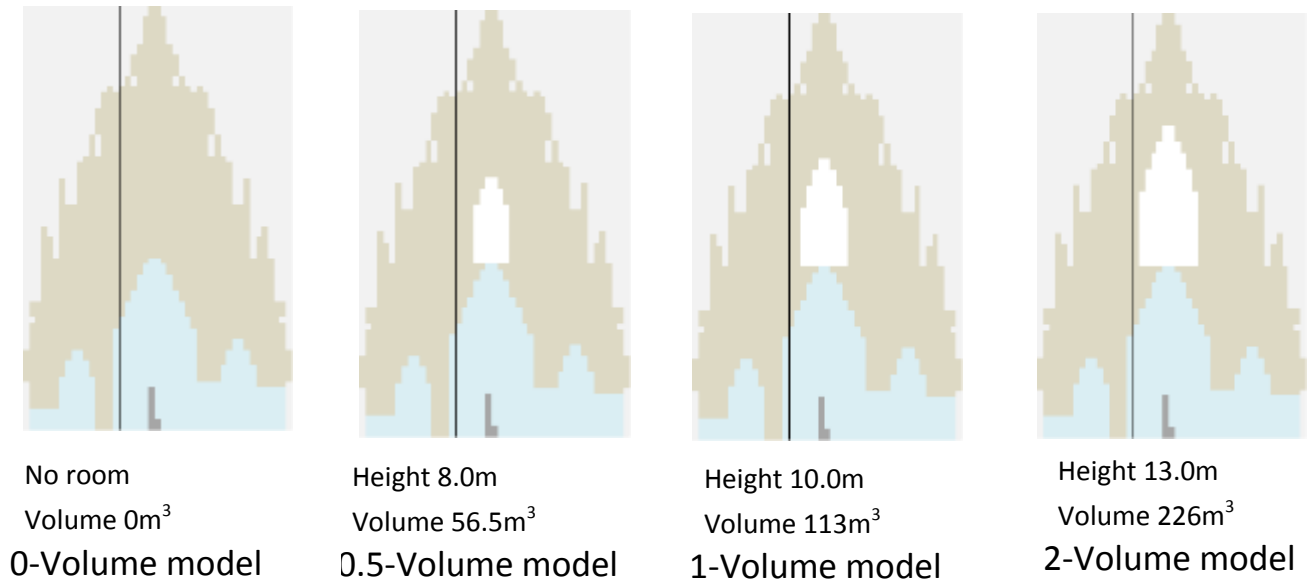


Fig.7 - Volume models assumed for simulation

### 2.3 Muon Monitoring Results

In order to cancel the detector characteristics, the ratios of the data before and after rotating the equipment shown in Fig.2 by 180 degrees were calculated. Table 1 shows the ratios of the data before the rotation to those after the rotation (= (before rotation) / (after 180-degree rotation around the vertical axis)). The horizontal line denotes the X direction (unit:  $10^{-3}$ rad), and the vertical row denotes the Y direction (unit:  $10^{-3}$ rad). When the value exceeds 1.0, it indicates that the muon flux is larger than the flux from opposite side of the direction of “before rotation”. For example, when the muon flux from a direction of (X,Y)=(-210 x  $10^{-3}$ rad, +280 x  $10^{-3}$ rad) (direction-1) is larger than that from (X,Y)=(+210 x  $10^{-3}$ rad, -280 x  $10^{-3}$ rad) (direction-2), the ratio (= (before rotation)/(after rotation) ) would exceed 1.0. The present table shows that there is less mass along direction-1 than that along direction-2.

y¥x	-210	-140	-70	0	70	140	210
280	1.1425	1.0073	0.913	1.0211	1.2113	1.1555	0.9793
210	1.2745	1.1059	1.1938	1.0607	1.1289	1.1108	1.2147
140	1.2842	1.0848	0.9849	0.9191	1.0228	0.9957	0.895
70	1.0495	1.1311	0.9892	0.9134	1.0501	0.9735	0.9052
0	0.9711	0.9601	0.9513	1.053	1.1058	0.9496	0.8646
-70	1.0245	1.0304	1.0931	0.9665	0.9242	0.906	0.7883
-140	1.1671	1.1317	1.0707	0.9809	0.9316	0.9178	0.8876
-210	1.1121	0.9902	1.0478	0.9854	0.9136	0.8578	0.7743
-280	0.9845	1.0155	0.9519	0.99	1.0318	0.8791	0.8488

Table 1 - Ratio of recorded data before and after rotation of equipment (unit of angle :  $10^{-3}$  rad)

### 2.4 Simulation Results

Utilizing the assumed models described in 2.2, the ratio of the data before the rotation and after the rotation was theoretically calculated by the same procedure on the assumption that the muon would penetrate in random direction and with random interval time. Tables 2 through 5 show the simulated ratio for the cases of 0-Volume, 0.5-Volume, 1-Volume and 2-Volume models, shown in Fig.7. In these tables, the elements of horizontal lines and vertical rows (bins) correspond to the segmental angle of the projection of muon detecting shown in Fig.4.

y\X	-210	-140	-70	0	70	140	210
280	0.952	0.73	0.677	0.775	1.014	1.12	1
210	0.909	0.732	0.611	0.658	0.987	1.133	0.962
140	0.771	0.638	0.521	0.552	0.838	0.971	0.827
70	0.656	0.534	0.48	0.596	0.909	1.055	0.938
0	0.703	0.622	0.694	1	1.441	1.608	1.423
-70	1.066	0.948	1.1	1.677	2.085	1.874	1.524
-140	1.209	1.03	1.193	1.81	1.919	1.567	1.297
-210	1.04	0.883	1.013	1.52	1.637	1.366	1.1
-280	1	0.892	0.986	1.29	1.476	1.371	1.05

Table 2 - Simulated ratio of 0-Volume model

y\X	-210	-140	-70	0	70	140	210
280	1.057	0.763	0.691	0.775	1.015	1.121	1
210	1.364	1.032	0.711	0.657	0.988	1.133	0.962
140	1.196	1.063	0.671	0.551	0.839	0.971	0.827
70	0.803	0.72	0.548	0.595	0.909	1.054	0.938
0	0.701	0.621	0.693	1	1.442	1.611	1.426
-70	1.067	0.949	1.1	1.68	1.825	1.389	1.245
-140	1.209	1.03	1.192	1.815	1.49	0.941	0.836
-210	1.04	0.883	1.013	1.522	1.407	0.969	0.733
-280	1	0.892	0.986	1.29	1.448	1.311	0.946

Table 3 - Simulated ratio of 0.5-Volume model

y\X	-210	-140	-70	0	70	140	210
280	1.158	0.888	0.731	0.774	1.015	1.121	1
210	1.408	1.106	0.743	0.656	0.988	1.132	0.962
140	1.322	1.069	0.666	0.551	0.839	0.971	0.827
70	1.081	0.85	0.618	0.594	0.911	1.057	0.94
0	0.786	0.688	0.731	1	1.367	1.453	1.273
-70	1.064	0.946	1.097	1.682	1.619	1.176	0.925
-140	1.209	1.03	1.192	1.815	1.501	0.936	0.757
-210	1.04	0.883	1.012	1.523	1.345	0.904	0.71
-280	1	0.892	0.985	1.291	1.369	1.126	0.864

Table 4 - Simulated ratio of 1-Volume model

y\X	-210	-140	-70	0	70	140	210
280	1.318	1.066	0.942	0.842	1.013	1.12	1
210	1.728	1.489	1.158	0.78	0.985	1.132	0.962
140	1.709	1.547	1.066	0.657	0.836	0.971	0.827
70	1.33	1.149	0.877	0.683	0.909	1.058	0.94
0	0.843	0.726	0.779	1	1.284	1.378	1.186
-70	1.063	0.946	1.1	1.465	1.14	0.87	0.752
-140	1.209	1.03	1.197	1.521	0.938	0.646	0.585
-210	1.04	0.883	1.015	1.282	0.864	0.672	0.579
-280	1	0.892	0.988	1.188	1.062	0.938	0.759

Table 5 - Simulated ratio of 1-Volume model

## 2.5 Comparison of Record and Simulation

We compared the recorded data shown in Table 1 with the simulation shown in Tables 2 through 5 (A total of 4 simulation cases among 6 cases are described in the present paper). The numbers of the bins meeting the following conditions were accounted as ;

$Ratio < 1$  ;  $0 \leq X \leq 210 \times 10^{-3} \text{ rad}$  and  $-280 \times 10^{-3} \text{ rad} \leq Y \leq 0$  : in the green frame (broken line)

$Ratio > 1$  ;  $-280 \times 10^{-3} \text{ rad} \leq X \leq 0$  and  $0 \leq Y \leq 280 \times 10^{-3} \text{ rad}$  : in the yellow frame (solid line)

As results, Fig. 8 shows the confidence level of recorded data in comparison with the simulation. The horizontal axis denotes the normalized volume of the assumed hidden room, while the vertical axis denotes the number of bins meeting the above-mentioned conditions. In Fig. 8,  $0\sigma$ ,  $1\sigma(68.3\%)$ ,  $2\sigma(95.5\%)$ ,  $3\sigma(99.7\%)$  denote reliability. This figure indicates that the possibility of existence of a hidden room being larger than 1-volume would exceed 90%. Furthermore, it should be noticed that the possibility of existence of a hidden room being larger than 2-volume model is in good agreement between simulation and record, which shows  $1\sigma$  standard deviation. This comparison means that the possibility of the existence of a hidden room being larger than 2-volume is approximately 70%. On the other hand, the possibility of existence of a hidden

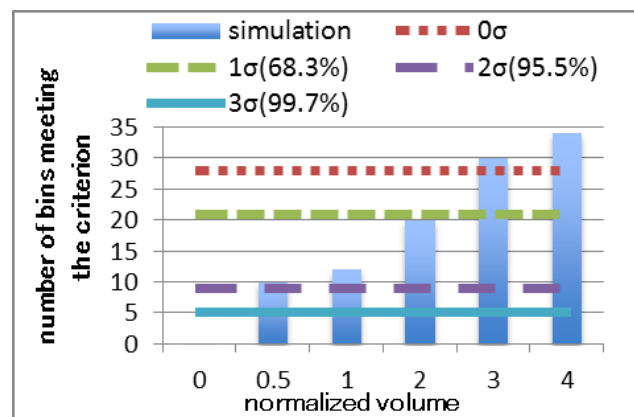


Fig.8 - Confidence level of data

room larger than 3-volumes was lower. It was concluded that the volume of the hidden room in the upper part of Candi Siva could be expressed by 2-volume model. Fig.9 displays the density profile of Candi Siva obtained from the muography in the present study. This new finding was taken into account to provide the analysis model for seismic evaluation in the next chapter.

### 3. Seismic Response Analysis

#### 3.1 Analysis Model

In our past studies, both the simplified lumped masses model and the 3-dimensional finite element model (See Fig.10) were employed [2][3]. In both models, dynamic soil-structure interaction was taken into account, as the natural frequency observed during not only the earthquake but also the microtremore measurements was good agreement with the analysis model in which the soil-structure interaction was taken into account. As introduced in Introduction, reinforced concrete structure was used to reconstruct the monument. To evaluate the earthquake-induced stress in the reinforced concrete frame and the inner rubble concrete, it would be more useful to employ the finite element model. Therefore, 3-dimensional finite element model was utilized in the present paper. Shown in Fig. 11, the finite element model was revised on the basis of the muography. Hence, the volume of the hidden room in the upper part of Candi Siva was enlarged to double volume shown in the sketch of the section (See Fig.5). Table 6 shows material properties of the structure used for the analysis. (Computer Code TDAP III was used.)

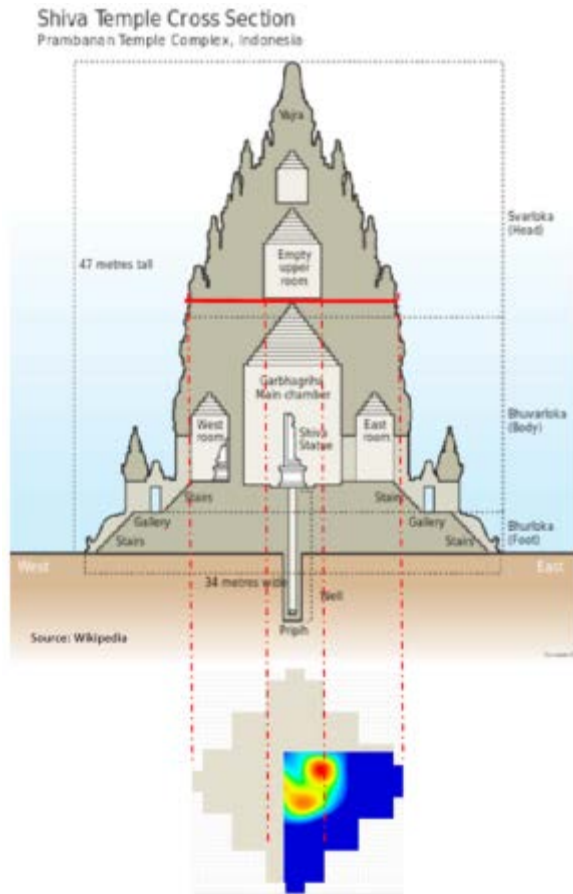


Fig.9 - Density profile of Candi Siva

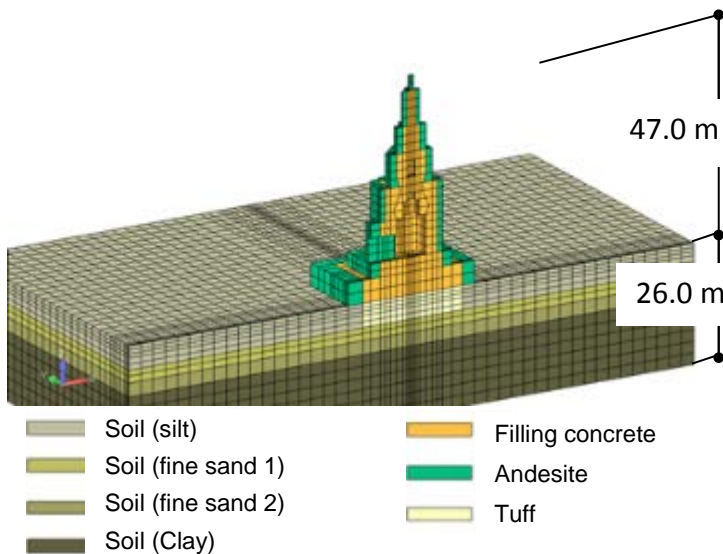


Fig.10 - 3-Dimensional finite element model of soil-structure system

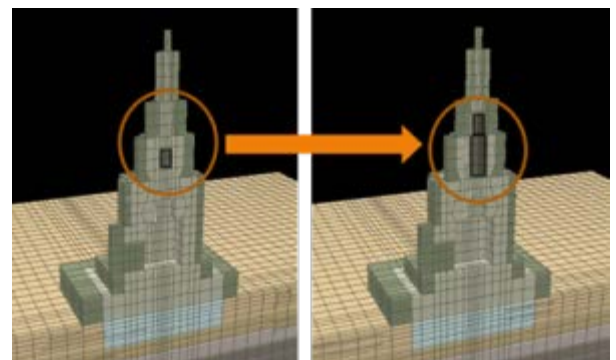


Fig. 11 - Revision of analysis model

Figs. 12 and 13 show the soil profile at the site and the inner reinforced concrete frame, respectively. The soil profile shown in Fig.12 was based on the surface wave profiling test and the standard penetration test. The inner reinforced concrete frame shown in Fig.13 was provided from the drawings prepared for reconstruction of Candi Garuda, because the size of the frame was able to be found in the drawings of Candi Garuda.

The analysis model was verified by comparison of the small earthquake records with the analysis, as the earthquake monitoring had been performed during 2010 and 2012 at Candi Siva. Some small earthquakes were recorded (Earthquakes on September 12, 2010, November 24, 2011 and March 19, 2012). Those earthquakes were described in our previous paper [3].

GL	-----	
-5m	Silt	$\rho = 1.8\text{g/cm}^3$ $V_s = 120\text{m/s}$
-8m	Fine sand	$\rho = 1.8\text{g/cm}^3$ $V_s = 260\text{m/s}$
-11m	Fine sand	$\rho = 1.8\text{g/cm}^3$ $V_s = 360\text{m/s}$
-26m	Clayey soil	$\rho = 1.7\text{g/cm}^3$ $V_s = 290\text{m/s}$
	Engineering bedrock sand	$\rho = 1.9\text{g/cm}^3$ $V_s = 400\text{m/s}$

Fig.12 - Soil profile model of surface layers

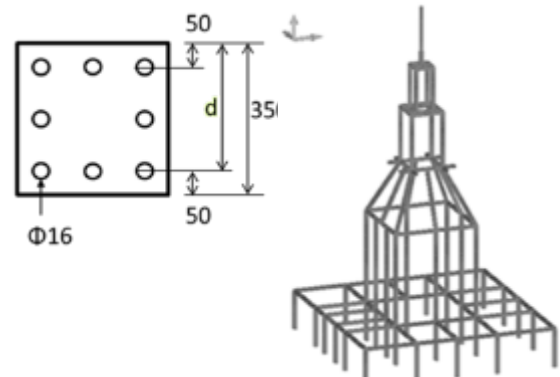


Fig.13 - Reinforced concrete frame

Table 6 - Material stiffness for analysis

Andesite ( $\text{N/mm}^2$ )	$1.8 \times 10^3$
Filling concrete ( $\text{N/mm}^2$ )	$1.6 \times 10^3$
RCC frame ( $\text{N/mm}^2$ )	$1.9 \times 10^3$
Tuff ( $\text{N/mm}^2$ )	$1.8 \times 10^3$

### 3.2 Input Earthquake Ground Motions

Note that earthquake ground motions should be essential for evaluation of seismic safety of heritage structures, however, the earthquake ground motions were not recorded in the vicinity of Prambanan Temple and in the epicentral area as well during the Central java Earthquake of 2006. Therefore, the ground motion level (PGV) was estimated to be approximately 10cm/s at the epicentral distance of 20-25km, being evaluated from the attenuation curve based on the earthquake records in the far-field. As the wave form utilized for the response analysis, the strong motions recorded during the past earthquakes of similar magnitude with severe damage to historical masonry buildings were appropriate to be used. The earthquake record of Athens Earthquake of September 7, 1999 was utilized in the present study [2]. Fig.14 shows the wave forms with the response spectrum of the input ground motion.

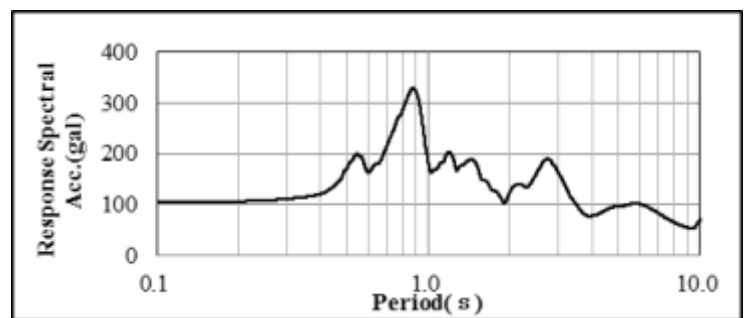
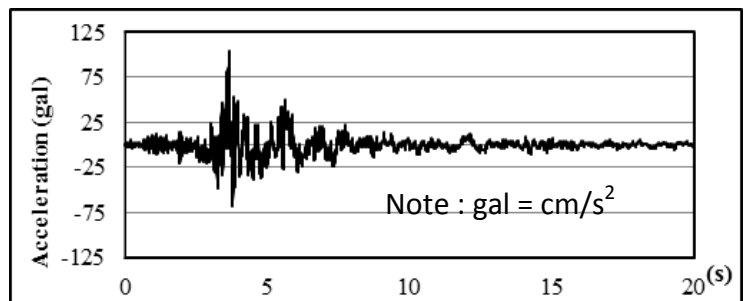


Fig.14 - Input ground motion

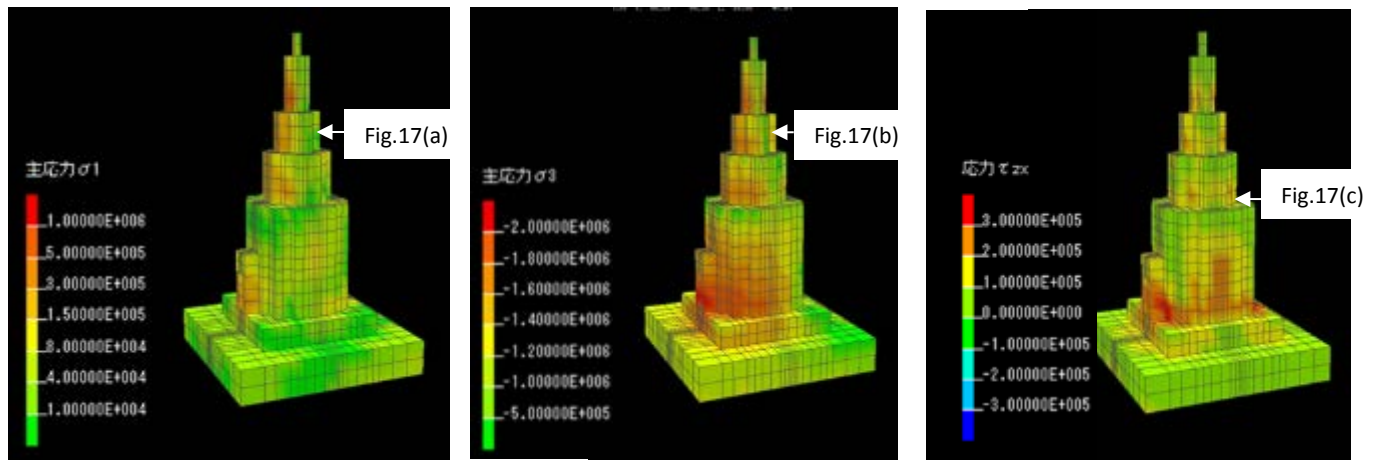
### 3.3 Analysis Results

Natural frequency of the soil-structure system of the revised model was 1.9Hz, being in good agreement of the microtremore record described in our past studies [1][2][3]. As results of the earthquake response analysis, Fig.15 shows the peak stresses ; tensile, compressive and shear stresses. The induced peak tensile stress was 1,270kN/m<sup>2</sup> at the base of the top roof. This peak tensile stress was less than the tensile strength of the andesite stones calculated to be 1,360kN/m<sup>2</sup> on the assumption that the tensile strength would be approximately 1/10 of the compressive strength evaluated from the material mechanical test using the new stones utilized for the restoration works. As well as, the earthquake-induced peak compressive stress induced, 2,220kN/m<sup>2</sup>, was less than the compressive strength of 13,600kN/m<sup>2</sup>. Those analysis results indicated that earthquake-induced stress was less than the inherent strength of the andesite stones, however, the tensile stress at some joints between stones might be subjected to the stress as high as the tensile strength during the earthquake, which might cause damage to the exterior walls. It should be also noticed in Fig. 15 that the earthquake-induced shear stress on the stone wall was concentrated at around the openings. On the other hand, it had been needed to judge if the inner concrete structure was damaged or not, for proposing structural restoration plan. Allowable flexural moment  $M_a$  was calculated from the following equation as ;

$$M_a = a_t \cdot f_t \cdot \frac{7}{8} \cdot d \quad (2)$$

Hence,  $a_t$ : sectional area of rein bar at tensile side,  $f_t$ : allowable tensile stress of rein bar,  $d$ : distance between gravity center of rein bar and end of section at tensile side.

At the roof top where the so-called whipping phenomenon was observed, the earthquake-induced peak flexural moment was calculated to be 12.6kNm, being less than the allowable moment of 30.8kNm given by Eq. (2).



(a) Peak tensile stress      (b) Peak compressive stress      (c) Peak shear stress

Fig. 15 - Induced peak stress

Furthermore, the stress induced at the corner of the hidden room is now focused and discussed. Fig. 16 shows the stresses induced at the elements around the hidden room, where stress of the elements arranged at the horizontal section are described at the height shown in Fig.15. Described in Fig. 16, compressive, tensile and stresses at the elements around the hidden room did not exceed their strength. Consequently, the earthquake-induced stress in the inner concrete structure and the inner hidden room were calculated to be less than the strength of the materials and allowable flexural moment, respectively. This finding given by the analysis indicated that it would not be needed to restore structurally the inner concrete structure and the stone walls around the hidden rooms.

#### 4. Concluding Remarks

Muography was successfully employed to know the size of the inner hidden room of Candi Siva, the Prambanan World Heritage Temple of masonry, damaged by Central Java Earthquake of 2006. The present study demonstrates that muography technique will be useful for non-destructive survey of masonry heritage structures of which inner structural conditions are unknown. After having grasped the condition of the inner hidden room of the monument, seismic structural analysis utilizing 3-dimensional finite element model of the soil-structure system was performed to make it clear whether the inner structure had been damaged or not by the earthquake. The analysis indicated that the inner structure of Candi Siva might not be structurally damaged. This finding contributed to go on the practical restoration project of this masonry monument.

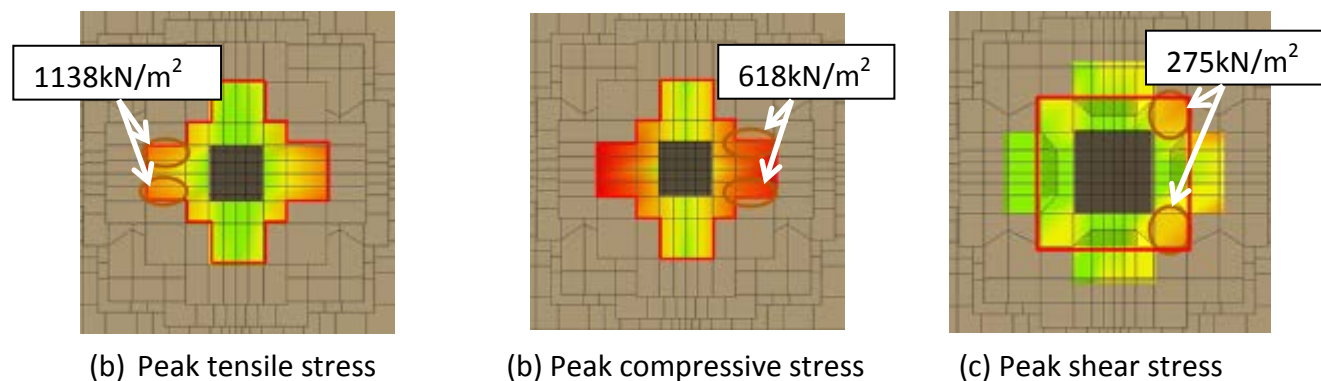


Fig. 16 - Induced peak stress around upper hidden room in horizontal section

#### Acknowledgements

The authors are deeply grateful to Dr. Harry Widiyanto, the General Directorate Archaeology and Museum, Direktur Pelestarian Cagar Budaya dan Permuseuman, Indonesia for his giving us excellent opportunity to perform the muon monitoring at the Prambanan Temple. The muon survey at the site was successfully performed in cooperation with staff of Archaeological Site office of Yogyakarta Special province. The present research was financially supported by Grants-in-Aid for Scientific Research, Japanese Governmental research fund in 2013 and 2014.

#### References

- [1] National Institute for Cultural Heritage., Japan Center for International Cooperation in Conservation National Research Institute for Cultural Properties, Tokyo. (2008). Research Cooperation on Conservational Restoration of the Cultural Heritage damaged by Central Java Earthquake –Reconstructive Supporting Report on the Prambanam World Heritage Site, 35-71
- [2] Hanazato T, Suprapt S, Subagio P, Uekita Y, Matsui T, Yamato S, Minowa C, Ono K, and Taneichi M (2010) : Seismic Assessment for Restoration of Prambanan World Heritage Temples Damaged by the Central Java Earthquake of 2006, Indonesia, Proc. of 8<sup>th</sup> International Masonry Conference, 1571-1580
- [3] Nakatani A, Hanazato T, Oyaizu N, Uekita Y, Minowa C, Ono K, Suprpto S and Subagio P (2012): Seismic Structural Performance of the Prambanan World Heritage Temple Damaged by the Central Java Earthquake of 2006 in Indonesia, Proc. of 15WCEE, Paper No.681
- [4] Tanaka H et al (2007) : High resolution imaging in the inhomogeneous crust with cosmic-ray muon radiography , the density structure below the volcanic crater floor of Mt. Asama, Japan, Science Direct, Earth and Planetary Science Letters 263, 104-113